

Raman scattering in $\text{YBa}_2\text{Cu}_3\text{O}_7$ single crystals: anisotropy in normal and superconductivity states

© M.F. Limonov¹, A.I. Rykov, S. Tajima, A. Yamanaka*

Superconductivity Research Laboratory, International Superconductivity Technology Center,
10–13, Shinonome 1-Chome, Koto-ku, Tokyo 135 Japah

* Research Institute for Electronic Science, Hokkaido University,
Sapporo 060 Japan

(Поступила в Редакцию 29 апреля 1997 г.
В окончательной редакции 2 октября 1997 г.)

Precise temperature and polarization dependencies of Raman spectra have been investigated for fully oxygenated twin-free $\text{YBa}_2\text{Cu}_3\text{O}_7$ single crystals. We have found a striking superconductivity — induced $x - y$ anisotropy in the temperature behavior of the 340 cm^{-1} line: the magnitudes of the softening and broadening are quite different in the xx - and yy -polarizations. This anisotropy suggests a contribution of the CuO -chain superconductivity with a pairing symmetry different from that for the CuO_2 plane, or indicates that the superconducting gap amplitudes are different in the k_x and k_y directions. The $d + s$ gap symmetry is the only realistic symmetry in the case of $\Delta_x \neq \Delta_y$.

1. Introduction: ten years later

Raman scattering spectra (RSS) provide an important information on the phononic and electronic excitations in the high- T_c superconductors and serves as a tool for testing the properties of the superconducting gap. Over the past ten years, a wealth of data was obtained on superconductivity-induced effects in the phonon behavior in $\text{YBa}_2\text{Cu}_3\text{O}_7$ (YBCO) crystals. Let us summarize main results obtained in the studies of the phononic RSS in the high- T_c materials. The first important one is related to the softening of the 340 cm^{-1} mode below T_c found by Macfarlane, Rosen and Seky on the polycrystalline samples in 1987, indicating a strong electron-phonon interaction (EPI) [1]. The softening of the 340 cm^{-1} mode was confirmed by many groups which measured on different states of YBCO including the ceramics, thin films and single crystals [2–4].

However, the linewidth anomaly depended critically on sample. Friedel et al. reported that the half-width at the half maximum (HWHM) of the 340 cm^{-1} line increased monotonically with lowering temperature in the superconducting state [5]. Other works [4,6] shown that the temperature dependence of the HWHM exhibited a maximum at intermediate temperatures $0 < T^* < T_c$. This maximum was considered to originate from a resonance of a phonon energy $h\nu$ to a superconducting gap energy $2\Delta(T)$ at $T = T^*$ [7]. Accordingly, this result is indicative of the gap energy at $T \rightarrow 0$ being larger than the phonon energy of 340 cm^{-1} ; $2\Delta(0) > 340 \text{ cm}^{-1}$.

Later, it was found that the 430 and 500 cm^{-1} A_g modes also show resembling anomalies, namely, additional hardening at $T < T_c$ [8–10].

In 1988, Zeyher and Zwicky (ZZ) have calculated theoretically the superconductivity-induced effects on the phonon self-energy at $q = 0$, by assuming an isotropic

s -wave gap and strong coupling for EPI [11,12]. According to the ZZ-model, the renormalization of the phonon self-energy results in softening for the phonons with frequencies $h\nu < 2\Delta(T)$ without a significant change of HWHM, whereas for the phonons with frequencies $h\nu > 2\Delta(T)$ the hardening accompanied with additional broadening of the linewidth is predicted. Friedl, Thomsen and Cardona have investigated the broadening of the B_{1g} -like modes in various $\text{RBa}_2\text{Cu}_3\text{O}_{7-\delta}$ compounds with different rare earth elements R [5]. With using the ZZ-model, they evaluated a value of the gap $2\Delta(0)$ to be 316 cm^{-1} ($2\Delta/kT_c \sim 5$), however, being smaller than the phonon energy 340 cm^{-1} .

A number of experimental studies were devoted in the ensuing period for attempting accurate determination of the temperature-dependent behavior of the 340 cm^{-1} mode and gap value $2\Delta(0)$, but the results are surprisingly different from each other. Altendorf et al. found that the 340 cm^{-1} mode exhibited no anomalous broadening below T_c , indicating $2\Delta(0)/kT_c = 5.9$ [9]. McCarty et al. reported the narrowing of the 340 cm^{-1} mode below T_c and, therefore, concluded a much larger value of the gap: $6.8kT_c < 2\Delta(0) < 7.7kT_c$ [10]. The attempts to reconcile the largely variable results were so far limited by the influence of impurities, defects and oxygen deficiencies. Thomsen et al. have shown that the temperature behavior of the 340 cm^{-1} line depends dramatically on the amount of defects in the samples [13]. Altendorf et al. [6] examined the superconductivity-induced change in the linewidths as a function of the oxygen content. Nevertheless on the basis of the ZZ-model, it is difficult to explain by the above factors all the differences of the RSS published in the literature.

Recently, Nicol, Jiang and Carbotte (NJC) have calculated the phonon-selfenergy effect for a d -wave pairing [14]. In contrast to the isotropic s -wave ZZ-model, NJC found that a phonon with $h\nu < 2\Delta(T)$ softens and broadens. The broadening take place just below T_c and shows a maximum at $T = T^*$; $h\nu = 2\Delta(T^*)$. The frequency ν exhibits a

¹ Permanent address: A.F. Ioffe Physical-Technical Institute, 194021 St. Petersburg, Russia

discontinuously change from hardening to softening at the same temperature T^* .

Another lacking ingredient of the majority RSS analyses is the overlooked importance of the orthorhombicity of the YBCO structure. The tetragonal approach for describing both superconducting gap and RSS was deviously implied or discussed explicitly in the large number of papers. However, McCarty et al. [15] have found that the 120, 150, 340 and 500 cm^{-1} A_g phonon lines exhibit significant anisotropy at room temperature, e.g., their lineshapes and peak frequencies are quite different in the xx -, yy - and zz -polarizations. This fact demonstrates the in-plane anisotropy of the EPI as well the out-of-plane one. Thus, we expect that some of the complicated phenomena observed in the RSS below T_c originate from the anisotropic properties of the superconducting order parameter.

We should note that, in spite of the large number of the experimental and theoretical works published during ten years since the first RSS studies were done on YBCO, several principal issues still remain unsolved. The most important and unsettled problems are summarized as follow.

1) No RSS study concerning the temperature dependencies of the out-of-plane and in-plane anisotropies are reported.

2) Although the in-plane anisotropy in the RSS at room temperature have already demonstrated [15] the limitation of the tetragonal approach, the validity and limitation of this approach to the superconducting induced phenomena have not been examined sufficiently.

3) No significant superconducting-induced effect has been observed in 120 and 150 cm^{-1} modes, although the condition $h\nu < 2\Delta(0)$ should be obviously held for these modes.

4) The temperature — dependent behavior of the 340 cm^{-1} mode is still controversial.

5) No RSS analysis was applied to examine the possible constraints imposed by the Raman experiment on the choice of the actual gap symmetry among pure isotropic s , anisotropic s , mixed $s + id$ and $s + d$ symmetries. This leads to the question about the possibilities of the phononic RSS in resolving the problem of pairing state symmetry and mechanism of superconductivity in high- T_c copper-oxides.

These issues which may be enlightening for the mechanism of the high- T_c superconductivity are addressed in the present study.

2. Experimental

1) Single crystal preparation and properties. The single crystal pulling technique developed in ISTECSRL (Tokyo), called as SRL-CP method [16], allowed one to prepare for the measurements a large number of crystals with different characteristics of twinning, oxygen content and impurity level. In order to avoid any influence of surface defects on RSS [17], the crystals were studied immediately after annealing or freshly

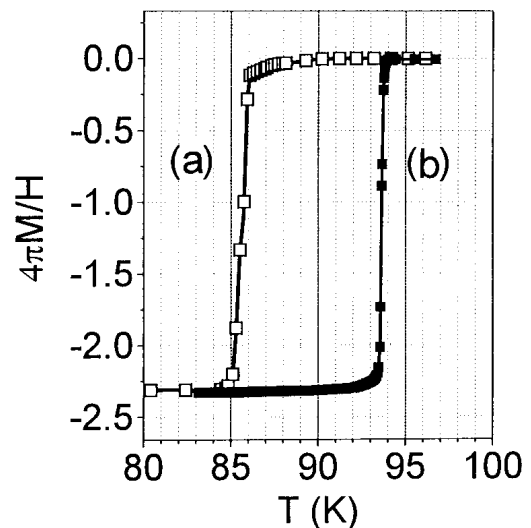


Figure 1. Superconducting transitions in overdoped ($T_c = 86\text{ K}$) (a) and optimally doped ($T_c = 93.6\text{ K}$) (b) twin-free YBCO single crystals measured in zero-field cooled samples at the applied field of 10 Oe. The estimated diamagnetization factor $D = 2.3$ correspond to $\chi = -1/4\pi$ in agreement with 100% shielding effect.

cleft just before the measurements. Another problem which has to be solved before collecting the reliable spectroscopic data is how to reduce the impurity concentration down to the p.p.m level. Because almost all cationic impurities in YBCO show large detrimental effect on T_c , the measurements of T_c were crucial for crystal selection. A large number of crystals were examined after detwinning process [18] and annealing at 490°C in the oxygen flow. For detwinning, the uniaxial pressure of typically 10 MPa was applied at cooling from 700° to 490°C during a week and, as a result, the formation of large untwinned orthorhombic crystals (a typical volume of 10 cm^3) with the oxygen content close to $\text{O}_{6.8}$ was obtained. The annealing temperature of 490°C results in optimal doping of the single crystals, whereas a lower anneal temperature leads to the overdoped state. Since the stoichiometric YBCO is overdoped [19–21] we avoid obtaining the overdoped state at the first state of oxygen loading, which is needed to select the purest crystals. The first step of sample preparation leads to optimal doping and allowed us to select for the study the crystals with maximum T_c of 93.6 K (Fig. 1).

The most important finding at the second step of sample preparation is that the apparent degree of overdoping could be much larger in the high-purity single crystals than, for instance, in ceramics or powder. This was again reflected in T_c value which indicate that the detrimental effect from oxygen overdoped into a single crystal is the most pronounced in the high quality single crystals. The latter effect could be understood from a simple idea that the lateral surface layer parallel to ab or ac plane in a small powder particle or single crystallite of granular material could be intrinsically oxygen-depleted or highly defective due to the effects of

surface [17]. Therefore, the powder or ceramic materials may show higher value of T_c when the measurement of T_c is done with using the surface-sensitive resistive method, or the low-field magnetic measurements, in which the screening current is induced in the surface layer of a small crystallite. With increasing field, the current capacity of such a thin surface layer becomes insufficient and the superconductive transition broadens for the granular material. Such a broadening occurs in the case when the powder or ceramic sample is overdoped in the bulk, but shows optimal T_c relevant to the surface. On the contrary, we observe in single crystals, which have a sharp transition, a small uniform shift of T_c with increasing field instead of the broadening of the superconductive transition. Since the surface contribution is negligible in the large crystals, the transition reflects the bulk oxygen content. These considerations are in consistent with the fact that the preparation process for the apparently optimally doped granular materials requires much lower temperature of annealing in the oxygen or in air [20] than that for genuinely optimally doped single crystals [21].

The importance of preparation of the overdoped crystals involves two reasons. One is that the close-to-ideal stoichiometric defect-free structure would exhibit the narrowest lines in the spectra. The other is that the anisotropic properties of YBCO are very different between the optimally doped and overdoped states [22]. In particular, the overdoped at 320°C sample show apparently twice reduced out-of-plane anisotropy $\gamma = (m_c/m_{ab})^{1/2}$, where m_c and m_{ab} are the effective carrier mass in the out-of-plane and in-plane directions, respectively. This could be roughly estimated from the slopes of irreversibility lines and fishtail lines [22]. A large difference of the in-plane anisotropies $\gamma = (m_a/m_b)^{1/2}$ between optimally doped and overdoped at 320°C was found in the normal state magnetic susceptibilities. The large in-plane anisotropy in the untwinned overdoped crystals is of particular interest in the present study. Thus, the best crystals were selected at the first stage of oxygen loading and then were annealed again at 320°C. As a result, the high quality samples with $T_c = 86$ K and transition width ΔT_c of 0.4 K (Fig. 1) were obtained.

2) Raman scattering technique. The RSS were studied with using a triple-stage spectrometer T64000 Jobin-Ivon equipped with a liquid-nitrogen cooled CCD detector. The typical spectral resolution was 3 cm^{-1} , and several spectra were measured with the resolution of 1 cm^{-1} . For accurately studying the temperature dependence of RSS and for eliminating the systematical error in the determination of frequency shifts, RSS was observed in the spectrograph mode, i.e. the spectral regime was fixed without scanning the diffraction gratings. The pseudobackscattering configuration was adopted. The xx - and yy -polarized RSS were obtained from the same portions on the mirrorlike regions of crystals. As for the zz -polarizations, the RSS taken from the ac and bc -surfaces, which were both native and cleft one, were essentially the same. The 514.5 nm line of Ar-ion laser was employed as an excitation light source. The power density was adjusted to be 0.2–1 W/cm²

on the sample surface, and, as result, the overheating was suppressed to be less than 3 K in all the experiments. To measure the temperature dependence of the RSS, the close-cycle UHV cryostat was used with temperature stabilization being better than 1 K. The spectra were corrected for the spectral response of the optical system and normalized for laser power.

3. Results and discussion

The RSS in the overdoped and optimally doped YBCO crystals at 290 K are shown in Fig. 2. Let us specify for the sake of clarity three spectral regions, comprising the lines at 120 and 150 cm^{-1} (low-frequency region), 340 cm^{-1} (mid-frequency region) as well as 430 and 500 cm^{-1} (high-frequency region). The rest of this paper is organized as follows: In Section 3.2 the temperature behavior of the 120 and 150 cm^{-1} modes (Fig. 3) is described; the RSS in the mid-frequency region and their analyses is presented in Section 3.3 (Figs. 4–6); in Section 3.4, the phonons in the high-frequency region is discussed; from these experimental results we analyzed superconducting gap symmetry in Section 3.5. Our discussion of the RSS is based on the results of the dynamical calculations [23], which showed quite satisfactory agreement with the experimental data and the calculations of other authors (see, for example, review [24]).

1) Raman scattering in optimally doped and overdoped YBCO crystals at room temperature. In Fig. 2, we can see a number of effects of varying the oxygen content of RSS. First, the frequencies of all the modes shift slightly. Second, the 234 and 583 cm^{-1} modes, which are observed in the yy -polarization in the optimally doped YBCO, vanish in the overdoped crystals. The appearance of these modes is related to the oxygen disorder at the Cu(1)–O(4)-chains. According to the dynamical calculations [23], in the fully stoichiometric YBCO the IR — active vibration of Cu(1) along the chains is at 153 cm^{-1} , and the corresponding chain oxygen mode is at 593 cm^{-1} . In the oxygen-deficient crystal these vibrations become Raman-active and appears in the yy -polarization (y axis is along the chains).

The distinctive features of the RSS in the overdoped crystals are well articulated polarization dependence and the absence of any additional line which is usually activated from oxygen disorder or impurity atoms, as mentioned above. The RSS shows only five well known vibrations of the A_g symmetry. Note that all the results presented below are relevant to the overdoped "O₇" crystals.

2) The 120 and 150 cm^{-1} A_g -modes. The 120 and 150 cm^{-1} A_g vibrations are formed mainly by z -displacements of Ba and planar Cu, respectively. According to Ref. [23], the atomic displacements at the Γ -point in the Brillouin zone at $T = 290$ K are as follows

$$120 \text{ cm}^{-1}: \quad 6\text{Ba} + 1\text{Cu} + 1\text{O}(2) + 1\text{O}(3), \quad (1)$$

$$150 \text{ cm}^{-1}: 9\text{Cu} + 3\text{O}(1) + 1\text{O}(2) + 1\text{O}(3), \quad (2)$$

where preceding the atoms coefficients denote corresponding normalized z -displacements; O(1) is the apical oxygen, O(2) and O(3) are the oxygens from the CuO_2 plane. Thus, admixture of z -displacements of other atoms is expected to be small.

As for the 120 cm^{-1} mode, we successfully observe the effect of the out-of-plane anisotropy of the electron-phonon interaction in the full temperature range between 10 K and 300 K (Fig. 3, *b*). This effect manifests itself in the significant difference of the peak frequencies between the out-of-plane zz -polarization and the planar xx - and yy -polarization. The anisotropic EPI is more clearly seen in the shape of the 120 cm^{-1} line (Fig. 2, *a*). In the yy -polarization, the line shape is strikingly asymmetric, being resulted from the coupling to the intense electronic background (Fano-type interference). On the other hand, in the zz -polarization, in which the electronic scattering at low frequencies is negligibly weak, the lineshape is symmetric and described well with a Lorentzian profile. As can be seen in Figs. 2, *a* and 3, *b*, the out-of-plane anisotropy is also apparent in the

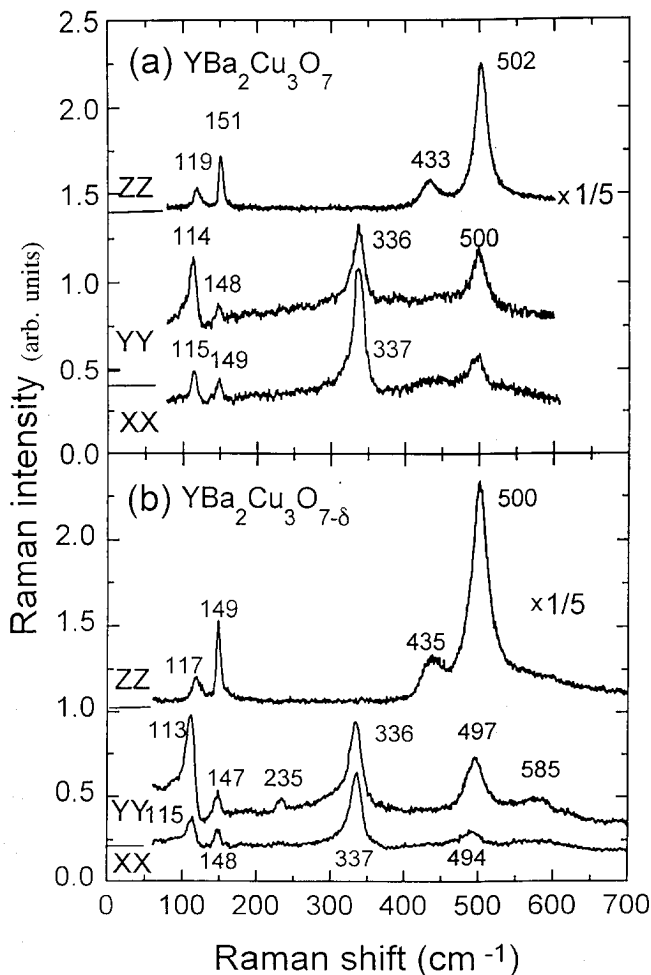


Figure 2. Raman spectra of the overdoped ($T_c = 86 \text{ K}$) (a) and optimally doped ($T_c = 93.6 \text{ K}$) (b) twin-free YBCO single crystals in the xx -, yy - and zz -polarizations at $T = 290 \text{ K}$.

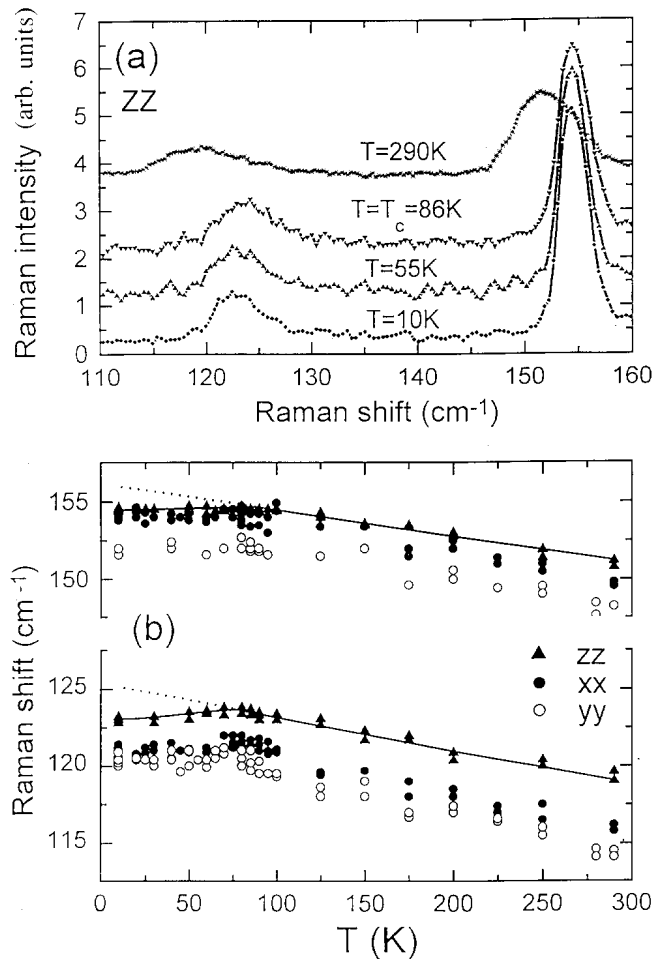


Figure 3. (a) Low-frequency region of RSS of the overdoped twin-free YBCO single crystals in zz -polarization at different temperatures above and below T_c . Shown in (b) are the temperature dependences of the 120 and 150 cm^{-1} modes in xx -, yy - and zz -polarizations. All lines are guides to the eye.

150 cm^{-1} mode (although not so conspicuous as for the 120 cm^{-1} mode).

One of the significant findings is the superconductivity-induced behaviour of the 120 and 150 cm^{-1} modes in xx , yy and zz -polarizations (Fig. 3, *b*). The 120 cm^{-1} mode frequency exhibits usual hardening with lowering temperature from 290 K to T_c . However below T_c this frequency slightly decreases. Therefore, superconductivity-induced softening of the 120 cm^{-1} mode takes place. As to the 150 cm^{-1} mode, it is almost temperature-independent below T_c . The softening of these modes lying below T_c entirely within the gap $h\nu < 2\Delta(0)$ was predicted by several theories [5,8]. It is noted that the successful observation of this effect is due to the narrow Raman lines in our high-quality samples. For example, the HWHM for the line at 150 cm^{-1} in zz -polarization is only 1.5 cm^{-1} at 10 K .

3) The 340 cm^{-1} B_{1g} -like mode. In the majority of studies of the superconductivity effects on the RSS in YBCO, the 340 cm^{-1} mode is the main target. In a crude

tetragonal assessment, this vibration has B_{1g} symmetry and corresponds to the out-of-phase displacements with equal amplitudes of the O(2) and O(3) oxygens in the direction of z-axis. In the genuine orthorhombic structure of the oxygen-undepleted YBCO, the symmetry of the 340 cm^{-1} mode turns into totally symmetric A_g one and the z-displacements of the O(2) and O(3) atoms are unequal [23]

$$340\text{ cm}^{-1} : 13\text{O}(2) - 12\text{O}(3). \quad (3)$$

The deviation from the ideal B_{1g} -vibrational configuration is small (below 10%). So this mode still has a B_{1g} character even in the orthorhombic YBCO, which is consistent with the polarization dependence reported in the literature.

Our key discovery deals with the character of softening of this mode. Because the relative magnitude of softening for the 340 cm^{-1} line is the largest one, it is possible to accurately measure the difference of its temperature behavior between the xx and yy polarizations. The results

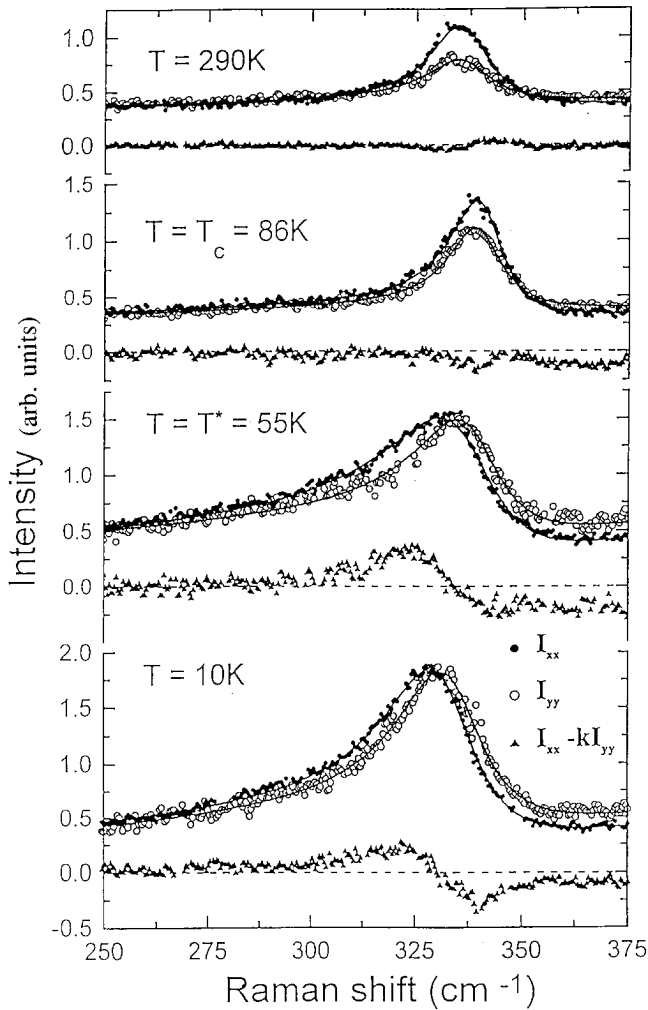


Figure 4. Raman spectra in the region of the 340 cm^{-1} mode at different temperatures in the xx - (solid circles) and yy -polarizations (open circles). The spectra are normalized to the intensity at 250 cm^{-1} . The filled triangles show the differential spectra $I_x - kI_y$ with the normalizing factor $k = I_x(\nu_x)/I_y(\nu_y)$.

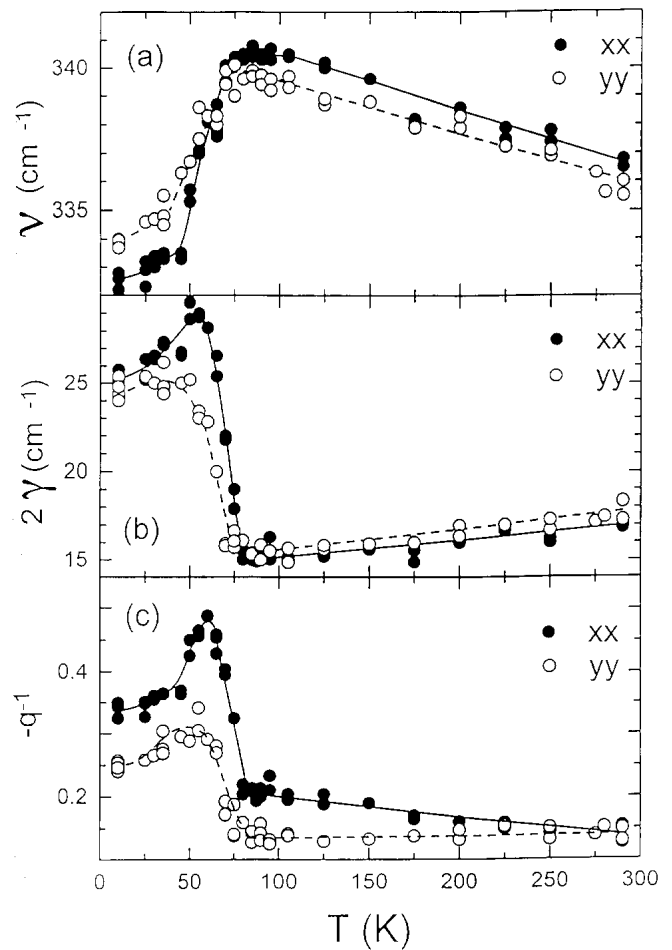


Figure 5. Temperature dependences of the frequency ν_α (a), the linewidth γ_α (b) and inverse asymmetry parameter $1/q_\alpha$ (c) for the 340 cm^{-1} line in the xx - and yy -polarizations. All lines are guides to the eye.

refer to the magnitude of softening and the character of broadening are illustrated in Figs. 4–6. We performed the least-squares fits to the RSS in a spectral region around the 340 cm^{-1} mode ($175\text{ cm}^{-1} < \nu < 400\text{ cm}^{-1}$) in terms of a standard expression

$$I = A + B\nu + C\nu^2 + I_0(\varepsilon + q)^2/(1 + \varepsilon^2), \quad (4)$$

where the term $A + B\nu + C\nu^2$ describes the background continuum arising from the electronic Raman scattering. The last term describes the Fano profile of the 340 cm^{-1} line where $\varepsilon = (\nu - \nu_\alpha)/\gamma_\alpha$ and q_α is the asymmetric parameter ($\alpha = x, y$). Here the frequency ν_α and linewidth γ_α are renormalized by the real and imaginary parts of the electronic response $\chi(\nu) = -R(\nu) + i\pi\rho(\nu)$ as $\nu_\alpha = \Omega + V^2R$ and $\gamma_\alpha = \Gamma + V^2\pi\rho$, respectively, where Ω and Γ are the uncoupled frequency and damping ($\Omega_x \equiv \Omega_y$, $\Gamma_x \equiv \Gamma_y$ for nondegenerated A_g -modes), and V is the coupling constant. It should be noted that the thermal Bose factor does not affect significantly the numerical fitting in the relevant frequency region.

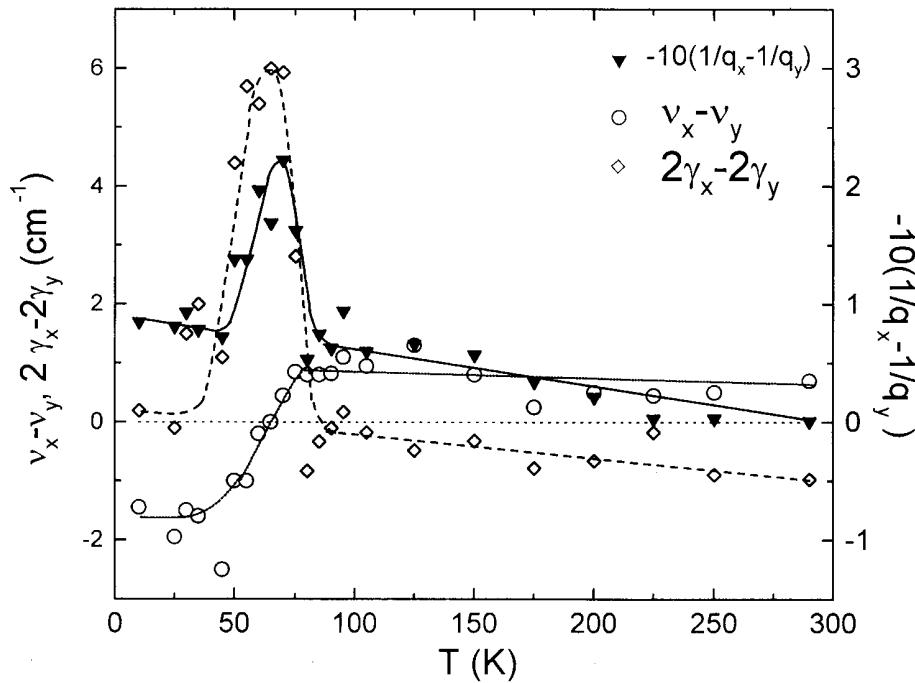


Figure 6. Temperature dependences of the $x - y$ differences of ν_α , γ_α , and $1/q_\alpha$ for the 340 cm^{-1} mode. All lines are guides for the eye.

In Fig. 4, the 340 cm^{-1} line is shown in the xx - and yy -polarizations together with the normalized differential spectra $I_x - kI_y$, which demonstrate clearly the in-plane anisotropy. In the normal state, the frequency of the 340 cm^{-1} line in the xx -polarization (ν_x) is slightly higher than that in the yy -polarization (ν_y) (Fig. 5, *a*). The difference $\nu_x - \nu_y$ is roughly temperature independent (Fig. 6) while the differences of the parameters γ and $1/q$ increase with decreasing temperature (Figs. 5, *b* and 5, *c*). Noticeably, we can see in Fig. 4 that the line shapes are almost symmetric in both polarizations at $T = 290 \text{ K}$, while at $T = T_c$ this line in the xx -polarization possess already a slight asymmetry.

At temperatures just below T_c , the frequency of the 340 cm^{-1} line deviates slightly from the T -linear dependence of the normal state one. With further lowering temperature this mode exhibits a steep softening. As for the xx -polarization, the frequency decreases by about 7 cm^{-1} in the temperature range of $40 < T < 70 \text{ K}$ whereas the decrease is only 1 cm^{-1} below 40 K . In the yy -polarization, the total softening of this line is about 5.5 cm^{-1} being smaller than that in the xx -polarization. Significantly, in the middle point of the main softening temperature range at $T_x^* = 55\text{--}60 \text{ K}$ there occurs the maximum broadening of this line in the xx -polarization, while in the yy -polarization, there is an uncertain maximum in the linewidth dependence at the temperature T_y^* about $45\text{--}50 \text{ K}$ (Fig. 5, *b*). The in-plane anisotropy of both the inverse line asymmetry $1/q$ and linewidth γ is quite large in the region $40 \text{ K} < T < T_c$ while the anisotropy is small again at low temperatures. As it can be seen from Fig. 3, the differential spectrum $I_x - kI_y$ turns out inverted when passing through T^* , demonstrating the changeover from $\nu_x > \nu_y$ above T^* to $\nu_y > \nu_x$ below T^* .

4) The 430 and 500 cm^{-1} A_g -modes. The 430 cm^{-1} vibration is mainly due to in-phase z -displacements of the O(2) and O(3) oxygens. While the displacements of O(2) and O(3) are equal in the oxygen-depleted tetragonal YBCO, in the orthorhombic structure this mode are accompanying the z -displacements of Cu(2) and O(1) as follows

$$430 \text{ cm}^{-1}: 12\text{O}(2) + 13\text{O}(3) - 1\text{Cu}(2) - 1\text{O}(1). \quad (5)$$

From Eqs. (3) and (5), it follows that the orthorhombic distortion mixes the tetragonal B_{1g} (O(2)–O(3)) and A_{1g} (O(2) + O(3)) modes belonging to the same A_g symmetry in D_{2h} structure. It is remarked that the distortion is very small for the 430 cm^{-1} A_g -vibration, as in the case for B_{1g} -like mode. As for the 500 cm^{-1} vibration, it is preferentially associated with the apical oxygen displacements along the z -axis:

$$500 \text{ cm}^{-1}: 17\text{O}(1) - 1\text{Cu}(2). \quad (6)$$

The temperature behaviors of the 430 and 500 cm^{-1} lines (Fig. 7) are similar to those reported previously [8–10]. The additional hardening of these lines takes place in the range between $T_c = 86$ and 40 K . The hardening of these modes indicates the magnitude of the superconducting gap being smaller than 430 cm^{-1} .

5) The symmetry of superconducting gap in $\text{YBa}_2\text{Cu}_3\text{O}_7$. In this Section, we first turn to the discuss of the general features of the effects of superconductivity on RSS. Next, we explore a possible origin of the in-plane anisotropy of the 340 cm^{-1} line and discuss the gap symmetry on the basis on the experimental data.

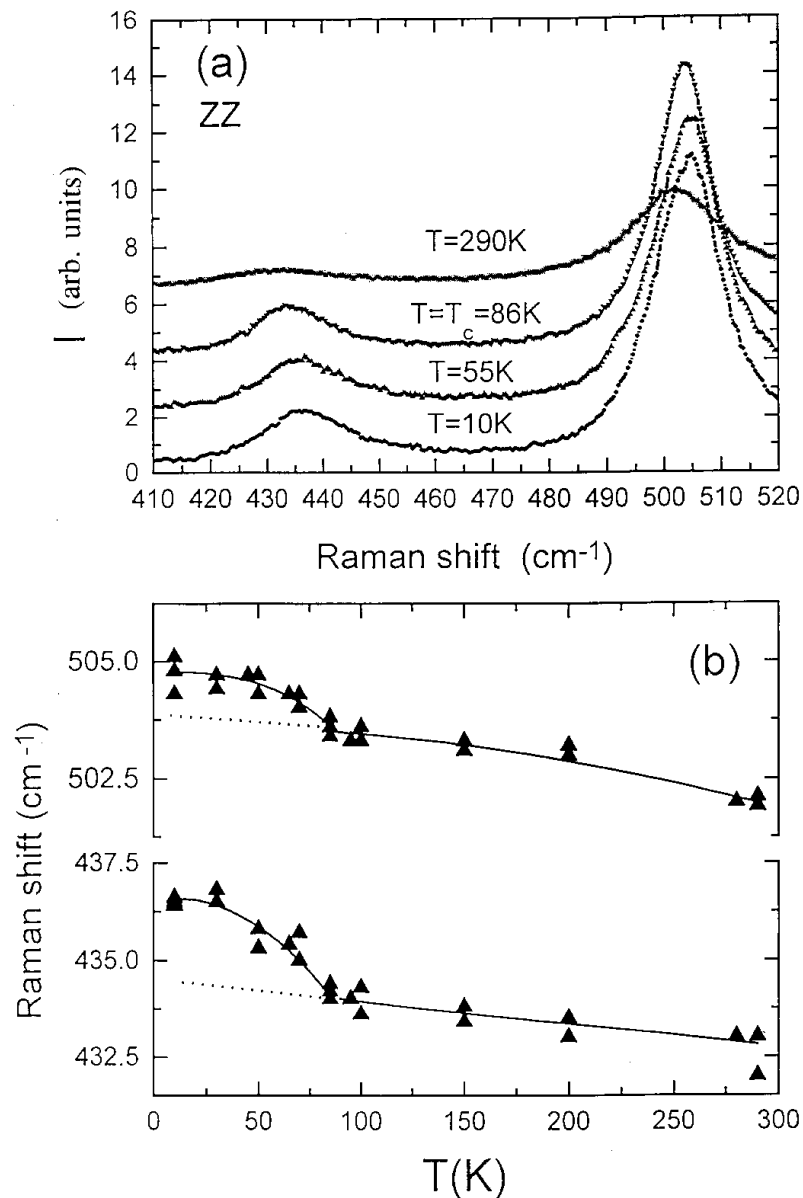


Figure 7. Temperature dependences of the RSS in high-frequency region (a) and for the frequencies of 430 and 500 cm^{-1} lines (b) in the zz -polarizations. All lines in panel (b) are only guides to the eye.

The main features of the selfenergy effects agree basically with those expected in a d -wave state [14]. Namely, the theory predicts that the step-like softening and maximum of the line broadening should be at the same temperature $T^* < T_c$ (Fig. 5, *a,b*). Actually, the temperature region of softening is broadened up to the appreciable width of 30 K (Fig. 5, *a*). This could be related with a significant width of the 340 cm^{-1} line, so that the 2Δ -peak of the density of states "crosses" this line in the finite temperature interval. On the other hand, the broadening of the 340 cm^{-1} line starts in both xx - and yy -polarizations immediately at the superconducting transition, again in accordance with the theoretical analysis [14].

Here we shall discuss the possible origin of the observed in-plane anisotropy in the RSS. According to the results of

the numerical calculations for the s -wave and d -wave states, the magnitude of softening is directly linked to the difference between phonon and gap energies, that is $2\Delta(T) - h\nu$. If the xx - and yy -polarized phonons probe predominantly the values of Δ_x and Δ_y , respectively, the $x-y$ anisotropy in the superconductivity-induced effects should result from difference of the gap values: $\Delta_x \neq \Delta_y$. Note that $\Delta_x = \Delta_y$ in all the cases of s^0 , s^+ , d , $s + id$ and $d + is$ symmetries with gaps of the forms:

$$\Delta^{s(0)} = \text{const}, \quad (7a)$$

$$\Delta^{s(+)} = \Delta^s (\cos k_x + \cos k_y), \quad (7b)$$

$$\Delta^d = \Delta^d (\cos k_x - \cos k_y), \quad (7c)$$

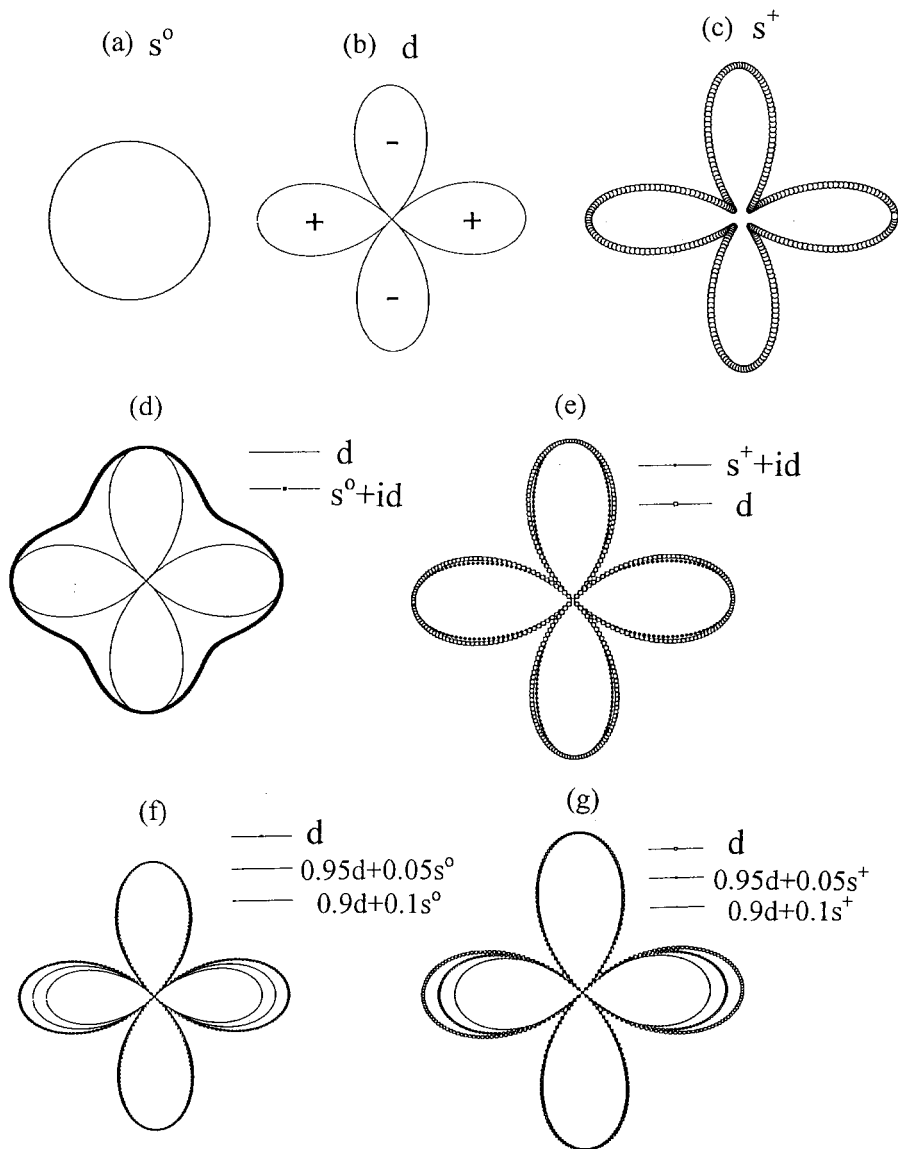


Figure 8. The gap functions for various ratios between the d - and s -component amplitudes. (a) — isotropic s^0 , (b) — d , (c) — anisotropic s^+ , (d) — d and mixed $s^0 + id$, (e) — d and mixed $s^+ + id$, (f) — d and mixed $0.95d + 0.05s^0$, $0.9d + 0.1s^0$, (g) — d and mixed $0.95d + 0.05s^+$, $0.9d + 0.1s^+$.

$$\Delta^{s+id} = \Delta^s(\cos k_x + \cos k_y) + i\Delta^d(\cos k_x - \cos k_y), \quad (7d)$$

$$\Delta^{d+is} = \Delta^d(\cos k_x - \cos k_y) + i\Delta^s(\cos k_x + \cos k_y). \quad (7e)$$

For the sake of explicitness, the functions (7b) and (7c) for the case of spherical Fermi surface with a radius of 0.7π (i.e. $k_x = 0.7\pi \cos \varphi$, $k_y = 0.7\pi \sin \varphi$, $0 \leq \varphi \leq 2\pi$) are depicted in Fig. 8. Clearly, no $x - y$ anisotropy is seen in the figure for both these functions. In this respect, it is pertinent to recall here the evolution of continuing debates on this gap symmetry problem. Mainly three periods in the chronology of events could be marked: 1) quick discard of the model of the isotropic s -gap; 2) the attempts of choice between the anisotropic s -gap vs d -gap; 3) extension of the number of the proposed models due to mixed $s + d$, $s + id$ and $d + is$ [25] symmetries and even due to coexistence of

two types of condensates with different order parameters of s and d symmetry [26].

A large variety of the experimental techniques have been used for determining the symmetry. Up until now, an emphatic progress has been reached in agreeing that the d -wave component could be predominant in the gap wave function. It has revealed, however, that the Ginzburg–Landau solution for the orthorhombic symmetry directly leads to the $d + s$ symmetry (or $s + d$ if the prevailing component is implied to be placed the first) [27–30]. The experimental conformation of the mixed symmetry are lacking yet. A possible exception could be related with a rationalization of the tunnel experiments by Dynes and co-workers [31], in which a current from Pb (s -wave superconductors) to YBCO was observed, although no such a current is expected in the

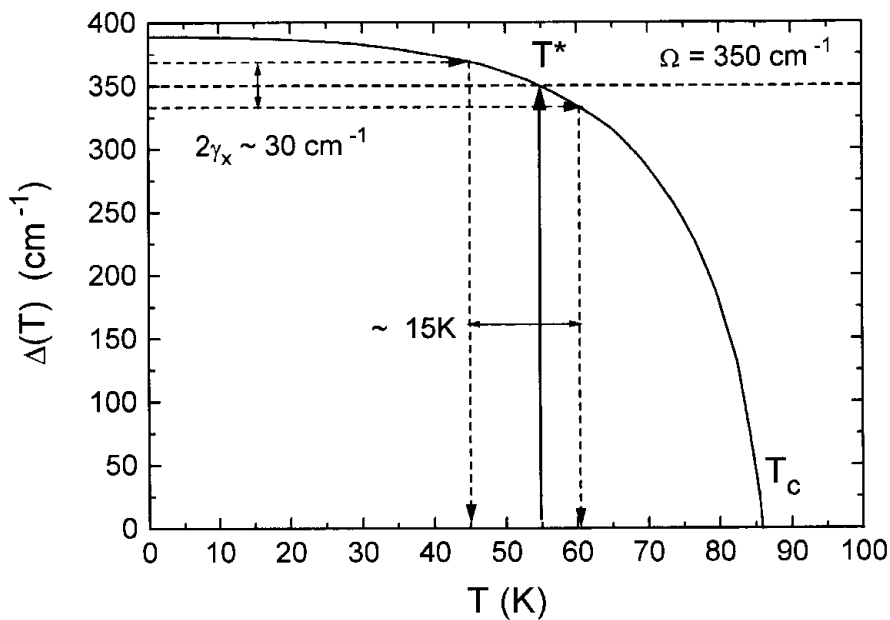


Figure 9. The BCS dependence of $\Delta(T)$ for $T_c = 86$ K and $\Delta(55 \text{ K}) = 350 \text{ cm}^{-1}$.

pure d -wave state. Thus, a possibility of an admixture of the s -wave component owing to orthorhombicity might be suggested for this observation [32,33].

In discussion of our experiments, an emphasis should be placed on the fact that the $d + s$ symmetry is the only realistic symmetry which applies to the case $\Delta_x \neq \Delta_y$. The $s + d$ state has a gap function of

$$\Delta^{d+s} = \Delta^d(\cos k_x - \cos k_y) + \Delta^s(\cos k_x + \cos k_y). \quad (8)$$

Fig. 8 shows the angular dependencies of the magnitude of the gap at the cylindrical Fermi surface with $k_x = 0.7\pi \cos \varphi$ and $k_y = 0.7\pi \sin \varphi$ for various ratios between the d and s component amplitudes. Because the main features of the RSS could be described in harmony with the d -wave model [14], the s -component is expected to be weaker than the d -component. The observation of the maximum $\gamma_x(T)$ near $T_x^* = 55$ K implies $2\Delta_x(55 \text{ K}) \cong \Omega$. In order to estimate a value of the uncoupled frequency Ω , one must analyze the observed spectrum in terms of a more complicated Green's function, taking into account of the ν -dependence of the electron-electron scattering rate $\tau(\nu)$ and mass $m(\nu)$. According to this analysis, $\Omega \cong 350 \text{ cm}^{-1}$ is larger than ν_α by about 10 cm^{-1} in the normal state. Assuming the BCS-like T -dependence of $\Delta(T)$, we obtain $2\Delta_x(0) = 400 \text{ cm}^{-1} = 6.7kT_c$ (Fig. 9). For the yy -spectrum, the maximum $\gamma_y(T)$ is observed around 45 K, $2\Delta_y(0) = 370 \text{ cm}^{-1} = 6.2kT_c$. Therefore, $2\Delta_x(0)/2\Delta_y(0) \cong 1.1$, which leads to a small amount of admixture of $\Delta_s \cong 0.05\Delta_d$ (Fig. 8).

Because of notable linewidth of the 340 cm^{-1} line, which is 30 cm^{-1} at $T^* = 55$ K, we can preclude broadening of the temperature range of softening and estimate the width of this region. By assuming the BCS dependence for

$\Delta(T)$, we obtain (Fig. 9) the width of the softening region being $\Delta T = 15$ K, which is quite comparable with the experimental value of 30 K (Fig. 5, *a*) broadened additionally due to a finite width of the 2Δ -peak of the electronic states density.

Now we shall discuss other possible explanation for the observed $x - y$ anisotropy in superconductivity-induced effects. It could be due to the CuO chain contribution. A coupling of the 340 cm^{-1} phonon with the chain electronic excitation is not expected to be strong, because this phonon mode does not involve vibrations of the atoms in the chain (see Eq. 3). However, the coupling could be enhanced by a resonance of this phonon energy and the interband excitation energy between the CuO chain and the CuO_2 plane bands. In this case, the 340 cm^{-1} phonon must be affected by the gap opening in the chain. If the chain superconductivity is induced mainly by the attractive interaction within the one-dimensional chain, the gap function cannot be a d -wave but should be a s -wave. Thus, the Raman response should be quite different from that for d -symmetry in the plane superconductivity. Consequently, the phonon self-energy effect is observed to be different in the yy -spectrum from that in the xx -spectrum which reflects only the d -gap in the plane.

4. Conclusions

The effect of the out-of-plane and the in-plane anisotropies, the softening below T_c of the 120, 150 and 340 cm^{-1} modes with frequencies $h\nu \leq 2\Delta(0)$ along with the well-known hardening of the 430 and 500 cm^{-1} modes with frequencies $h\nu > 2\Delta(0)$, the determined bounded region of softening for the 340 cm^{-1} mode coinciding in

temperature with the maximum broadening of this line constitute the entire picture of the phonon behavior in the superconducting phase of YBCO.

It is remarkable that when a variety of the experimental techniques were until now used for determining the symmetry, the main goal was focused on the searching for the nodes of the gap functions and the investigation of the behavior of the phase of the order parameter at a 90° rotation around z -axis. From the results of Raman experiment we have succeeded to examine the symmetry of the gap in a quite different manner. We compared the magnitudes of the gap along the crystal axes x and y , in which not minima but maxima of the $\Delta(k)$ gap function are expected i.e. we compared the amplitudes of the order parameter at a 90° rotation around z -axis. Neither the ZZ pure s -model [11,12] nor the NJC pure d -model [14] cannot consistently explain the presented results, which are hopefully uplifting for an impetus in further development of theory.

One of the plausible candidates for the origin of the observed $x-y$ anisotropy in both broadening and softening for the 340 cm^{-1} mode is the $d+s$ gap symmetry. We have deduced the gap value along the x -axis $2\Delta_x(0) = 6.7kT_c$ and along the y -axis $2\Delta_y = 6.2kT_c$. The value of $x-y$ anisotropy of the gap value is significant ($2\Delta_x(0) - 2\Delta_y(0) = 0.5kT_c$), so that the admixture of the s -component is about 5%.

Another possibility for explanation of the $x-y$ anisotropy is an independent superconducting channel in the CuO chain with a different pairing symmetry from that of the CuO₂ plane superconductivity. In this case, the anisotropy could be attributed to the contribution of the chain superconductivity in the yy -spectrum.

Finally, it should be emphasized that the issue of gap symmetry might be intimately related to the physical origin of pairing interactions. It is well known that the s -wave is likely linked with long-range interactions and implies the phononic mechanism. On the other hand the d -wave pairing arises from the spin-fluctuation mechanism [34]. It might be then inspiring to speculate that the mechanism of the superconductivity in YBa₂Cu₃O_{7-x} crystals originates from the mixed interactions.

The authors thank A.G. Panfilov, R. Eder, Yu.E. Kitaev and V.P. Smirnov for their helpful discussions.

This work was supported by NEDO for the R&D of Industrial Science and Technology Frontier Program.

References

- [1] R.M. Macfarlane, H.J. Rosen, H. Seki. Solid State Commun. **63**, 831 (1987).
- [2] A. Wittlin, R. Liu, M. Cardona, L. Genzel, W. Konig, W. Bauhofer, H. Mattausch, A. Simon. Solid State Commun. **64**, 477 (1987).
- [3] R. Feile, U. Schmitt, P. Leiderer, J. Schubert, U. Poppe. Z. Phys. **B72**, 161 (1988).
- [4] S.L. Copper, F. Slakey, M.V. Klein, J.P. Rice, E.D. Bukowski, D.M. Ginsberg. Phys. Rev. **B38**, 11 934 (1988).
- [5] B. Friedl, C. Thomsen, M. Cardona. Phys. Rev. Lett. **65**, 915 (1990).
- [6] E. Altendorf, X.K. Chen, J.C. Irwin, R. Liang, W.N. Hardy. Phys. Rev. **B47**, 8140 (1993).
- [7] S.L. Copper, F. Slakey, M.V. Klein, J.P. Rice, E.D. Bukowski, D.M. Ginsberg. J. Opt. Soc. Am. **B6**, 436 (1989).
- [8] C. Thomsen, M. Cardona, B. Friedl, C.O. Rodriguez, I.I. Mazin, O.K. Andersen, Solid State Commun. **75**, 219 (1990).
- [9] E. Altendorf, J. Chrzanowski, J.C. Irwin, A. O'Reilly, W.N. Hardy. Physica **C175**, 47 (1991).
- [10] K.F. McCarty, H.B. Radousky, J.Z. Liu, R.N. Shelton. Phys. Rev. **B43**, 13 751 (1991).
- [11] R. Zeyher, G. Zwicknagl. Solid State Commun. **66**, 617 (1988).
- [12] R. Zeyher, G. Zwicknagl. Z. Phys. **B78**, 175 (1990).
- [13] C. Thomsen, B. Friedl, M. Cieplak, M. Cardona. Solid State Commun. **78**, 727 (1991).
- [14] E.J. Nicol, C. Jiang, J.P. Carbotte. Phys. Rev. **B47**, 8131 (1993).
- [15] K.F. McCarty, J.Z. Liu, R.N. Shelton, H.B. Radousky. Phys. Rev. **B41**, 8792 (1990).
- [16] Y. Yamada, S. Shiohara. Physica **C217**, 182 (1993).
- [17] A.I. Rykov, M.F. Limonov, S. Tajima. In: Advances in Superconductivity IX / Ed. S. Nakajima and M. Murakami. Springer Verlag, Tokyo (1997). P. 391.
- [18] A.I. Rykov, W.J. Jang, H. Unoki, S. Tajima. In: Advances in Superconductivity VIII / Ed. H. Hayakawa and Y. Enomoto. Springer Verlag, Tokyo (1996). P. 341.
- [19] J. Tallon, N.E. Flower. Physica **C204**, 237 (1993).
- [20] A.N. Lavrov. Physica **C216**, 36 (1993).
- [21] S. Miyamoto, Y. High, J. Schutzmann, H. Kutami, S. Tajima, Y. Shiohara. In: Advances in Superconductivity VII / Ed. K. Yamafuji and T. Morishita. Springer Verlag, Tokyo (1995). P. 129.
- [22] A.I. Rykov, S. Tajima. In: Critical Currents in Superconductors / Ed. T. Matsushita and K. Yamafuji. World Scientific, Singapore (1996). P. 369.
- [23] Yu.E. Kitaev, M.F. Limonov, A.G. Panfilov, R.A. Evarestov, A.P. Mirgorodsky. Phys. Rev. **B49**, 9933 (1994).
- [24] Yu.E. Kitaev, M.F. Limonov, A.P. Mirgorodsky, A.G. Panfilov, R.A. Evarestov. Phys. Sol. Stat. **36**, 475 (1994).
- [25] G. Kotliar. Phys. Rev. **B37**, 3664 (1988).
- [26] K.A. Muller. Nature **377**, 133 (1995).
- [27] Q.P. Li, B.E.C. Koltenbah, R. Joynt. Phys. Rev. **B48**, 437 (1993).
- [28] C. O'Donovan, J.P. Carbotte. Phys. Rev. **B52**, 16 208 (1995).
- [29] C. O'Donovan, J.P. Carbotte. J. Low Temp. Phys. **105**, 495 (1996).
- [30] K. Maki, M.T. Beal-Monod. Phys. Lett. **A208**, 365 (1995).
- [31] A.G. Sun, D.A. Gajevski, M.B. Maple, R.C. Dynes. Phys. Rev. Lett. **72**, 2267 (1994).
- [32] M. Sigrist, T.M. Rice. Rev. Mod. Phys. **67**, 503 (1995).
- [33] D.J. van Harlingen. Rev. Mod. Phys. **67**, 515 (1995).
- [34] D. Pines. Physica **C185**, 120 (1991).